

Particle entry through reconnection grooves in the magnetopause with a dawnward IMF as simulated by a 3-D EM particle code

K.-I. Nishikawa

Department of Physics and Astronomy, Louisiana State University, Baton Rouge, LA 70803

Abstract. We report progress in the long-term effort to represent the interaction of the solar wind with the Earth's magnetosphere using a three-dimensional electromagnetic particle code. After a quasi-steady state is established with an unmagnetized solar wind we gradually switch on a northward interplanetary magnetic field (IMF), which causes a magnetic reconnection on the magnetopause tailward of the dayside cusps and makes the magnetosphere dipolarized. In the case that the northward IMF is switched gradually to dawnward, there is no signature of reconnection in the near-Earth magnetotail in contrast to the case with the southward turning. On the contrary analysis of magnetic fields in the magnetopause confirms a signature of magnetic reconnection at both the dawnside and duskside. The plasma sheet in the near-Earth magnetotail clearly thins as in the case of southward turning. Arrival of dawnward IMF to the magnetopause creates a reconnection groove which causes particle entry into the deep region of the magnetosphere via field lines that go near the magnetopause. This deep connection is more fully recognized tailward of Earth. The flank weak-field region joins onto the plasma sheet and the current sheet to form a geometrical feature called the cross-tail S that structurally integrates the magnetopause and the tail interior. This structure might contribute to direct entry between the magnetosheath plasma to plasma sheet, in which the entry process heats the magnetosheath plasma to plasma sheet temperatures. In spite of strong plasma entry into the inner magnetosphere, the dawnward IMF prevents the reconnection in the near-Earth magnetotail due to the penetrated IMF By component. Therefore, the onset of substorms may not take place. However, it is still possible that this particle entry causes pseudo-substorm onsets.

Introduction

Studies of ionospheric convection patterns in the dayside high-latitude region demonstrate that the IMF B_y component gives rise to a dawn-dusk asymmetry [Cowley *et al.*, 1991; Fujimoto *et al.*, 1997; Cumnock *et al.*, 1997; and references therein]. When IMF B_y is, say, negative (dawnward), the reconnected flux tubes are accelerated azimuthally, such that those connected to the southern (northern) hemisphere move duskward (dawnward) [e.g., Gosling *et al.*, 1990; Cowley *et al.*, 1991; Khurana *et al.*, 1996]. As a result, the flux tubes will enter the magnetotail from two open quadrants, north-dusk and south-dawn. In order to establish the above

scenario, we have studied how the reconnected field lines are transported towards the tail.

In this letter, we report new results with a dawnward IMF which show reconnection from the cusps through the flanks which facilitates the magnetosheath particle entry into the plasma sheet directly, which is consistent with observations [e.g., Fujimoto *et al.* 1997, and references therein].

Simulation Model and Results

This code [Buneman, 1993] utilizes charge-conserving formulas [Villasenor and Buneman, 1992] and radiating boundary conditions [Lindman, 1975]. We have used the same initial and boundary conditions used in our previous work [for details, see Nishikawa, 1997, 1998].

At step 768 [Buneman *et al.*, 1992, 1995; Nishikawa *et al.*, 1995] a northward IMF ($B_z^{IMF} = 0.2$), (for comparison, average B at the dayside magnetopause ($\approx 10R_E$) is nearly 2.8) is switched on, and the northward-IMF front reaches about $x = 120\Delta$ at step 1280. The Alfvén velocity with this IMF is $v_A/c = 0.05(\bar{n}_i)^{-1/2} = 0.05$ for the average ion density $\bar{n}_i = 1$. At step 1217 the northward IMF was switched to dawnward. In this case the amplitude of the IMF is kept constant and the IMF was rotated counter clockwise (viewed from the Sun).

The magnetic field lines at time step 1728 are plotted in Fig. 1, (a) in the three-dimension, and the projections (b) on the xz plane (c) on the yz plane, and (d) on the xy plane. The dawnward IMF connects to the north dayside cusp and extends from the south dayside cusp towards the dawnside. Later, more dawnward IMF will connect with the magnetospheric field along the flank.

In order to check the interaction of the dawnward IMF with the magnetic field near the Earth, Fig. 2 shows cross-sectional slices (viewed from the tail; the duskside is left) of the total magnetic field $|\mathbf{B}|$ at three x positions (a) $67\Delta(\approx 3R_E)$, (b) $71\Delta(\approx -1R_E)$, (c) $73\Delta(\approx -3R_E)$, and (d) the electron thermal energy at $x = 71\Delta(\approx -1R_E)$. The Earth is located at $(y, z) = (47.5, 48)$. It should be noted that in Figs. 2a, 2b, and 2c the maximum and minimum values are set in order to highlight the very weak magnetic field islands. With other diagnostics at different x positions such as Figs. 2a, 2b, and 2c, the simulation results show that distinctive regions of very weak magnetic field emanate from the regions of dayside cusps and radiate tailward [White *et al.*, 1998]. The null lines (reconnection grooves) lie in the very weak magnetic field islands as shown in the three consecutive slices (Figs. 2a, 2b, and 2c). For example, at $x = 73\Delta(\approx -3R_E)$ as shown in Fig. 2c, the null lines (reconnection grooves) are located at $(y, z) = (36\Delta, 42\Delta)(\approx (11R_E, -6R_E))$ and =

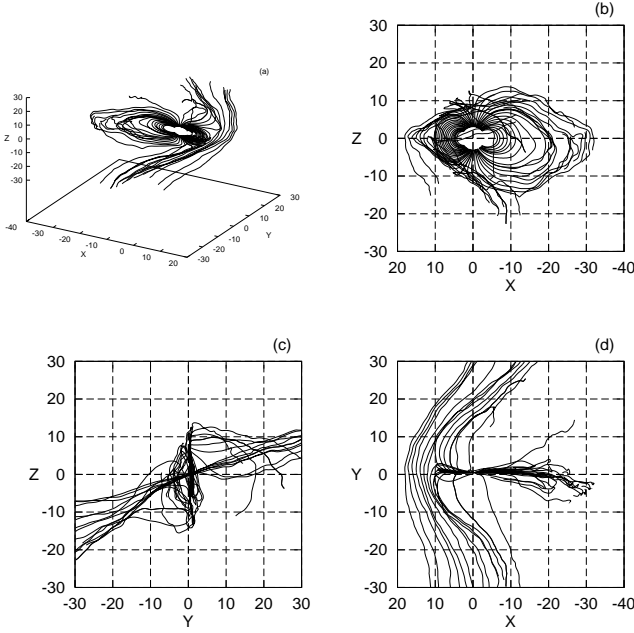


Figure 1. Magnetic field lines at step 1728 are shown (a) in the three-dimension from the dawnside, and the projections (b) on the xz plane (c) on the yz plane, and (d) on the xy plane.

$(58\Delta, 57\Delta) (\approx (-11R_E, 9R_E))$. Combining the two plates shown in Figs. 2b and 2d (at $x = 71\Delta (\approx -1R_E)$), one can see that the reconnection groove (Fig. 2b) is an access region for magnetosheath plasma [White *et al.*, 1998]. It is also a heating region for the plasma (electrons) as shown in Fig. 2d (duskside) indicating a large dawn-dusk asymmetry in the near-Earth magnetosphere (e.g., [Cumnock *et al.*, 1997]). In Fig. 2d, through the groove $((y, z) = (37\Delta, 41\Delta) (\approx (10R_E, -7R_E)))$ magnetosheath plasma (electrons) has ac-

cess to the deep regions of the magnetosphere via field lines that go near the magnetopause and is heated (e.g., [Ohtani *et al.*, 1995]). Other figure (not shown here) shows that deep connection between the magnetopause flank weak-field region begins already on the dayside [White *et al.*, 1998]. However, this deep connection is most fully recognized tailward of Earth, where it is best seen in cross-sectional views of the tail as shown in Fig. 3.

Figure 3 shows a cross-section of the tail at $x = 85\Delta (\approx -15R_E)$ viewed from the tail [e.g., Kaymaz *et al.*, 1995; Walker and Ogino, 1996]. (The subsolar line is located at $(y, z) = (47.5, 48)$.) Contours of B_x is shown in Fig. 3a, which outlines the tail and shows the northern (dark blue) and southern (dark red) lobes. The neutral line is defined by the condition $B_x = 0$. Note that the neutral sheet is well defined across the midplane of the tail, as expected, but that it also extends as a (sharply) defined feature along the southern dusk and northern dawn flanks (not so clear), which confirms the observation presented in White *et al.* [1998]. The extended current sheet has a sigmoid shape. This geometrical structure is referred to as the cross-tail S [White *et al.*, 1998]. The flank parts of the cross-tail S lie in the flank, weak-field region which is extended from the dayside magnetopause [White *et al.*, 1998]. Other aspects of the cross-tail S are also seen in the contours of field strength ($|\mathbf{B}|$) as shown in Fig. 3b. Note the two islands of very weak field $((y, z) = (31\Delta, 35\Delta) (\approx (16R_E, -13R_E))$ and $(66\Delta, 64\Delta) (\approx (-18R_E, 16R_E))$ that seem to mark the point on each flank where the tail part of the cross-tail S joins the magnetopause null lines (see also the islands of very weak magnetic field in Figs. 2a, 2b, and 2c). The thermal energy ($E_{th}^j = 0.5 * \Sigma m_j (v^j - v_d^j)^2$, where $v_d^j = \Sigma v^j / \Sigma$ and $j = i, e$ of ions (Fig. 3c) and electrons (Fig. 3d) are shown. The region of elevated ion temperature associated with the flank null lines $((y, z) = (31\Delta, 35\Delta) (\approx$

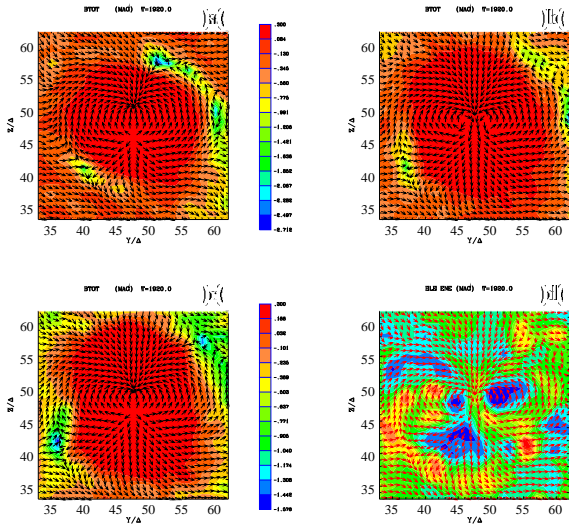


Figure 2. Dusk-dawn cross-sectional slices of the the total magnetic field $|\mathbf{B}|$ at three x positions (a) $67\Delta (\approx 3R_E)$, (b) $71\Delta (\approx -1R_E)$, (c) $73\Delta (\approx -3R_E)$, and (d) the electron thermal energy at $x = 71\Delta (\approx -1R_E)$ at time step 1920. The arrows show the magnetic field, which strength has been scaled in order to make field direction clearer for weak fields. Therefore, the length of the vectors is not a true presentation of the field magnitude.

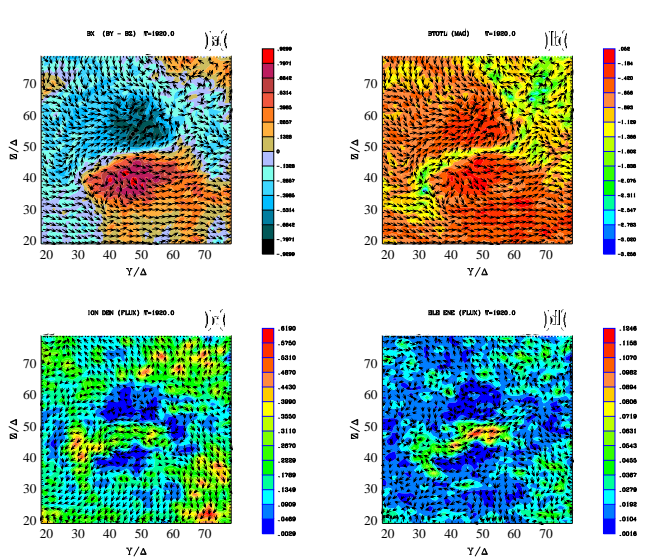


Figure 3. Dusk-dawn cross section of the tail at $x = 85\Delta (\approx -15R_E)$ is shown at time step 1920; (a) B_x with the magnetic field, (b) the total magnetic field ($|\mathbf{B}|$) with the magnetic field, (c) the ion thermal energy with ion average velocity, and (d) the electron thermal energy with electron average velocity. All arrows are scaled.

($16R_E$, $-13R_E$), the dawnside is not so clear) is evidently in geometrical connection with the plasma sheet as revealed here as a cross-tail bar of elevated ion temperature (located between the cold ion lobes (dark blue) as shown in Fig. 3c). The elevated ion temperature domains (around $(y, z) = (30\Delta, 41\Delta) (\approx (17R_E, -7R_E))$) describe the figure of the cross-tail S (The dawnside is not so clear). This feature is also seen in the electron temperature, however, the highest temperature is located in the center of plasma sheet ($(y, z) = 48\Delta, 47\Delta) (\approx (-1R_E, -1R_E))$ as shown in Fig. 3d.

As expected from the large particle entry (shown in Fig. 2d), electrons are injected into the inner magnetosphere from the duskside magnetopause which is also shown in the equatorial plane at the same time step (1920). Comparing with the previous time step (1728), the electron density is increased by about two times in the near-Earth magnetotail. Furthermore, the inner edge is moved from $79\Delta (\approx -9R_E)$ to $75\Delta (\approx -5R_E)$. The magnetic field in the duskside magnetopause (around $(x, y) = (70\Delta, 40\Delta) (\approx (0.5R_E, 7R_E))$) becomes disturbed, which corresponds to the reconnection groove. It should be noted that the electron density in the noon-midnight cross section at the same time step shows no reconnection in the near-Earth magnetotail. This may be explained by the fact that the penetrated IMF B_y component (as shown by the arrows in Figs. 3a and 3b) stabilize the tearing instability (The IMF with finite B_y increases the yy component of the electrical conductivity sharply above a critical B_y/B_z) [Hernandez et al., 1993; Ono et al., 1996]. Consequently, the reconnection does not take place in the near-Earth magnetotail. Therefore, the onset of substorms may not take place. However, particle injection takes place through the reconnection groove at the duskside magnetopause, which may be related to pseudo-substorm onsets (e.g., [Ohtani et al., 1995]).

Discussion

The results presented in Figures 1 through 3 show that even with the modest grid-size of 215 by 95 by 95 cells, our 3-D fully kinetic model is able to generate the interesting results with the dawnward IMF. The simulation results show that, due to the dawnward IMF, magnetic reconnection takes place on the flanks of the dayside magnetopause [e.g., Baker et al. 1996; Fujimoto et al. 1996, 1997]. On each flank, the null line runs tailward from a position near the dayside cusp. A fan of weak field emanates from the region of the dayside cusp and radiates tailward with the null line as its polarward border. The flank weak-field fan joins onto the plasma sheet and the current sheet to form a geometrical feature called the cross-tail S that structurally integrates the magnetopause and the tail interior [White et al., 1998]. This structure might be a channel of direct entry between the magnetosheath plasma to plasma sheet, in which the entry process heats the magnetosheath plasma to plasma sheet temperatures. At this time step, no reconnection takes place in the near-Earth magnetotail due to the penetrated IMF B_y component (as shown by the arrows in Figs. 3a and 3b) [Hernandez et al., 1993; Ono et al., 1996]. The new geometrical features confirmed by the 3-D EM particle code (i.e. the flank, weak-field fan and the cross-tail S) are seen also in maps compiled from IMP 8 data taken at $30 R_E$ down the tail [e.g., Kaymaz et al., 1995; Walker and

Ogino, 1996].

These preliminary simulation results with the dawnward IMF suggest that the IMF B_y component is very important for plasma entry [Cowley et al., 1991; Fedder et al., 1995; Kaymaz et al., 1995; Ohtani et al., 1995; Khurana et al., 1996; Walker and Ogino, 1996; Nishida et al., 1996; Baker et al., 1996; Fujimoto et al., 1996, 1997; White et al., 1998; and references therein]. The penetrated IMF B_y component stabilize the tearing instability, consequently it prevents the reconnection in the near-Earth magnetotail. Therefore, we believe that the IMF B_y component is important to determine the timing and intensity of substorms as described in the last section. Further simulations will be performed by selecting sets of time-varying solar wind conditions (especially direction). As shown in Fig. 2d, the particle entry through the duskside magnetopause with the IMF B_y component seems to contribute to “theta aurora” [e.g., Cumnock et al. 1997; Chang et al. 1998].

The more realistic results reported here suggest that full 3-D electromagnetic particle simulations will become an important tool for the theoretical understanding of Earth’s magnetosphere in the not-so-distant future. For the present, however, scaling and grid size remain substantial problems. However, some form of scaling is usually needed in particle simulations, even in one and two dimensions, and still such simulations are able to reveal much of the physics behind natural phenomena.

Acknowledgments. We thank W. White, G. Siscoe, S. Ohtani, and W. Horton for useful discussions. The development of the simulation code was performed at the National Center for Supercomputing Applications, University of Illinois at Urbana-Champaign and the production runs were performed at Pittsburgh Supercomputing Center. Both centers are supported by the National Science Foundation.

References

- Baker, D. N., et al., A possible interpretation of cold ion beams in the Earth’s tail lobe, *J. Geomag. Geoelectr.*, **48**, 699, 1996.
- Buneman, O., TRISTAN: The 3-D, E-M Particle Code, in *Computer Space Plasma Physics, Simulation Techniques and Software*, edited by H. Matsumoto and Y. Omura, Terra Scientific, Tokyo, p. 67, 1993.
- Buneman, O., T. Neubert, and K.-I. Nishikawa, Solar wind-magnetosphere interaction as simulated by a 3D, EM particle code, *IEEE Trans. Plasma Sci.*, **20**, 810, 1992.
- Buneman, O., K.-I. Nishikawa, and T. Neubert, Solar wind-magnetosphere interaction as simulated by a 3D EM particle code, *Space Plasmas: Coupling Between Small and Medium Scale Processes*, ed. M. Ashour-Abdalla, T. Chang, and P. Dusenbery, AGU Geophys. Monograph, **86**, p. 347, 1995.
- Chang, S.-W., et al., A comparison of a model for the theta aurora with observations from Polar, Wind, and SuperDARN, *J. Geophys. Res.*, in press, 1998.
- Cowley, S. W. H., J. P. Morell, and M. Lockwood, Dependence of convective flows and particle precipitation in the high-latitude dayside ionosphere on the X and Y components of the interplanetary magnetic field, *J. Geophys. Res.*, **96**, 5557, 1991.
- Cumnock, J. A., et al., Evolution of the global aurora during positive IMF B_z and varying IMF B_y conditions, *J. Geophys. Res.*, **102**, 17,489, 1997.
- Fedder, J. A., et al., Topological structure of the magnetotail as a function of interplanetary magnetic field direction, *J. Geophys. Res.*, **100**, 3613, 1995.
- Fujimoto, M., et al., Plasma entry from the flanks of the near-Earth magnetotail: GEOTAIL observations in the dawnside LLBL and the plasma sheet, *J. Geomag. Geoelectr.*, **48**, 711, 1996.

- Fujimoto, M., et al., Dayside reconnected field lines in the south-dusk near-tail flank during an IMF $B_y > 0$ dominated period, *Geophys. Res. Lett.*, *24*, 931, 1997.
- Gosling, J. T., et al., Plasma flow reversals at the dayside magnetopause and the origin of the asymmetric polar cap convection, *J. Geophys. Res.*, *95*, 8073, 1990.
- Hernandez, J. W., W. Horton, and T. Tajima, Low-frequency mobility response functions for the central plasma sheet with application to tearing modes, *J. Geophys. Res.*, *98*, 5893, 1993.
- Kaymaz, Z., et al., Interplanetary magnetic field control of magnetotail field: IMP 8 data and MHD model compared, *J. Geophys. Res.*, *100*, 17,163, 1995.
- Khurana, K. K., R. J. Walker, and T. Ogino, Magnetospheric convection in the presence of interplanetary magnetic field B_y : A conceptual model and simulations, *J. Geophys. Res.*, *101*, 4907, 1996.
- Lindman, E. L., Free-space boundary conditions for the time dependent wave equation, *J. Comp. Phys.*, *18*, 66, 1975.
- Nishida, A., et al., Magnetotail convection in geomagnetically active times 2. Dawn-dusk motion in the plasma sheet, *J. Geomag. Geoelectr.*, *48*, 503, 1996.
- Nishikawa, K.-I., Particle entry into the magnetosphere with a southward IMF as simulated by a 3-D EM particle code, *J. Geophys. Res.*, *102*, 17,631, 1997.
- Nishikawa, K.-I., Reconnections at near-Earth magnetotail and substorms studied by a 3-D EM particle code, *Global Observations and Models in the ISTP Era*, ed. J. L. Horwitz, W. K. Peterson, and D. L. Gallagher, AGU Geophys. Monograph, in press, 1998.
- Nishikawa, K.-I., O. Buneman, and T. Neubert, Solar Wind-Magnetosphere Interaction as Simulated by a 3-D EM Particle Code, *Astrophys. Space Sci.*, *227*, 265, 1995, also in *Plasma Astrophysics and Cosmology*, edited by A. T. Peratt, Kluwer Academic Pub., p. 265, 1995.
- Ohtani, S., et al., Four large-scale field-aligned current system in the dayside high-latitude region, *J. Geophys. Res.*, *100*, 137, 1995.
- Ono, Y., et al., Ion acceleration and direct ion heating in three-component magnetic reconnection, *Phys. Rev. Lett.*, *76*, 3328, 1996.
- White, W., et al., The magnetospheric sash and the cross-tail S, *Geophys. Res. Lett.*, *25*, This issue, 1998.
- Villasenor, J., and O. Buneman, Rigorous charge conservation for local electromagnetic field solvers, *Comp. Phys. Comm.*, *69*, 306, 1992.
- Walker, R. J. and T. Ogino, A global magnetohydrodynamic simulation of the origin and evolution of magnetic flux ropes in the Magnetotail, *J. Geomag. Geoelectr.*, *48*, 765, 1996.

Ken-Ichi Nishikawa, Department of Physics and Astronomy, Louisiana State University, Baton Rouge, LA 70803, (e-mail: kenichi@rouge.phys.lsu.edu)

(Received September 22, 1997; revised December 3, 1997; accepted February 12, 1998.)